Teppo Luukkonen

Modelling and control of quadcopter

School of Science

Mat-2.4108
Independent research project in applied mathematics

Espoo, August 22, 2011

Aalto University
School of Science

Contents

1 Introduction

Quadcopter, also known as quadrotor, is a helicopter with four rotors. The rotors are directed upwards and they are placed in a square formation with equal distance from the center of mass of the quadcopter. The quadcopter is controlled by adjusting the angular velocities of the rotors which are spun by electric motors. Quadcopter is a typical design for small unmanned aerial vehicles (UAV) because of the simple structure. Quadcopters are used in surveillance, search and rescue, construction inspections and several other applications.

Quadcopter has received considerable attention from researchers as the complex phenomena of the quadcopter has generated several areas of interest. The basic dynamical model of the quadcopter is the starting point for all of the studies but more complex aerodynamic properties has been introduced as well [1, 2]. Different control methods has been researched, including PID controllers [3, 4, 5, 6], back-stepping control [7, 8], nonlinear $\mathcal{H}_\infty$ control [9], LQR controllers [6], and nonlinear controllers with nested saturations [10, 11]. Control methods require accurate information from the position and attitude measurements performed with a gyroscope, an accelerometer, and other measuring devices, such as GPS, and sonar and laser sensors [12, 13].

The purpose of this paper is to present the basics of quadcopter modelling and control as to form a basis for further research and development in the area. This is pursued with two aims. The first aim is to study the mathematical model of the quadcopter dynamics. The second aim is to develop proper methods for stabilisation and trajectory control of the quadcopter. The challenge in controlling a quadcopter is that the quadcopter has six degrees of freedom but there are only four control inputs.

This paper presents the differential equations of the quadcopter dynamics. They are derived from both the Newton-Euler equations and the Euler-Lagrange equations which are both used in the study of quadcopters. The behaviour of the model is examined by simulating the flight of the quadcopter. Stabilisation of the quadcopter is conducted by utilising a PD controller. The PD controller is a simple control method which is easy to implement as the control method of the quadcopter. A simple heuristic method is developed to control the trajectory of the flight. Then a PD controller is integrated into the heuristic method to reduce the effect of the fluctuations in quadcopter behaviour caused by random external forces.

The following section presents the mathematical model of a quadcopter. In the third section, the mathematical model is tested by simulating the quadcopter with given control inputs. The fourth section presents a PD controller to stabilise the quadcopter. In the fifth section, a heuristic method including a PD controller is presented to control the trajectory of quadcopter flight. The last section contains the conlusion of the paper.

2 Mathematical model of quadcopter

The quadcopter structure is presented in Figure 1 including the corresponding angular velocities, torques and forces created by the four rotors (numbered from 1 to 4).

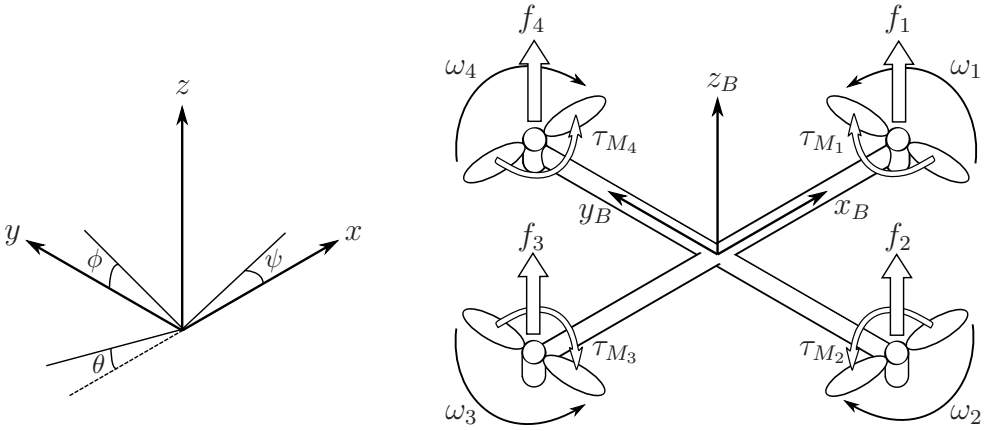

Figure 1: The inertial and body frames of a quadcopter

The absolute linear position of the quadcopter is defined in the inertial frame x,y,z-axes with $\boldsymbol{\xi}$. The attitude, i.e. the angular position, is defined in the inertial frame with three Euler angles $\boldsymbol{\eta}$. Pitch angle θ determines the rotation of the quadcopter around the y-axis. Roll angle ϕ determines the rotation around the x-axis and yaw angle ψ around the z-axis. Vector $\boldsymbol{q}$ contains the linear and angular position vectors

$$\boldsymbol{\xi} = \begin{bmatrix} x \\ y \\ z \end{bmatrix}, \quad \boldsymbol{\eta} = \begin{bmatrix} \phi \\ \theta \\ \psi \end{bmatrix}, \quad \boldsymbol{q} = \begin{bmatrix} \boldsymbol{\xi} \\ \boldsymbol{\eta} \end{bmatrix}. \tag{1}$$

The origin of the body frame is in the center of mass of the quadcopter. In the body frame, the linear velocities are determined by $\boldsymbol{V}_B$ and the angular velocities by $\boldsymbol{\nu}$

$$\boldsymbol{V}_B = \begin{bmatrix} v_{x,B} \\ v_{y,B} \\ v_{z,B} \end{bmatrix}, \quad \boldsymbol{\nu} = \begin{bmatrix} p \\ q \\ r \end{bmatrix}. \tag{2}$$

The rotation matrix from the body frame to the inertial frame is

$$\boldsymbol{R} = \begin{bmatrix} C_\psi C_\theta & C_\psi S_\theta S_\phi - S_\psi C_\phi & C_\psi S_\theta C_\phi + S_\psi S_\phi \\ S_\psi C_\theta & S_\psi S_\theta S_\phi + C_\psi C_\phi & S_\psi S_\theta C_\phi - C_\psi S_\phi \\ -S_\theta & C_\theta S_\phi & C_\theta C_\phi \end{bmatrix}, \tag{3}$$

in which $S_x = sin(x)$ and $C_x = cos(x)$. The rotation matrix $\boldsymbol{R}$ is orthogonal thus $\boldsymbol{R}^{-1} = \boldsymbol{R}^{\mathrm{T}}$ which is the rotation matrix from the inertial frame to the body frame.

The transformation matrix for angular velocities from the inertial frame to the body frame is $\boldsymbol{W}_\eta$, and from the body frame to the inertial frame is $\boldsymbol{W}_\eta^{-1}$, as shown in [14],

$$\begin{aligned} \dot{\boldsymbol{\eta}} &= \boldsymbol{W}_\eta^{-1}\,\boldsymbol{\nu}, \qquad \begin{bmatrix} \dot{\phi} \\ \dot{\theta} \\ \dot{\psi} \end{bmatrix} = \begin{bmatrix} 1 & S_\phi T_\theta & C_\phi T_\theta \\ 0 & C_\phi & -S_\phi \\ 0 & S_\phi/C_\theta & C_\phi/C_\theta \end{bmatrix} \begin{bmatrix} p \\ q \\ r \end{bmatrix}, \\ \boldsymbol{\nu} &= \boldsymbol{W}_\eta\,\dot{\boldsymbol{\eta}}, \qquad \begin{bmatrix} p \\ q \\ r \end{bmatrix} = \begin{bmatrix} 1 & 0 & -S_\theta \\ 0 & C_\phi & C_\theta S_\phi \\ 0 & -S_\phi & C_\theta C_\phi \end{bmatrix} \begin{bmatrix} \dot{\phi} \\ \dot{\theta} \\ \dot{\psi} \end{bmatrix}, \end{aligned} \tag{4}$$

in which $T_x = tan(x)$. The matrix $\boldsymbol{W}_\eta$ is invertible if $\theta \neq (2k-1)\phi/2, (k \in \mathbb{Z})$.

The quadcopter is assumed to have symmetric structure with the four arms aligned with the body x- and y-axes. Thus, the inertia matrix is diagonal matrix $\boldsymbol{I}$ in which $I_{xx} = I_{yy}$

$$\boldsymbol{I} = \begin{bmatrix} I_{xx} & 0 & 0 \\ 0 & I_{yy} & 0 \\ 0 & 0 & I_{zz} \end{bmatrix}. \tag{5}$$

The angular velocity of rotor i, denoted with ω_i, creates force f_i in the direction of the rotor axis. The angular velocity and acceleration of the rotor also create torque τ_{M_i} around the rotor axis

$$f_i = k\,\omega_i^2, \quad \tau_{M_i} = b\,\omega_i^2 + I_M\,\dot{\omega}_i, \tag{6}$$

in which the lift constant is k, the drag constant is b and the inertia moment of the rotor is I_M. Usually the effect of $\dot{\omega}_i$ is considered small and thus it is omitted.

The combined forces of rotors create thrust T in the direction of the body z-axis. Torque $\boldsymbol{\tau}_B$ consists of the torques τ_ϕ, τ_θ and τ_ψ in the direction of the corresponding body frame angles

$$T = \sum_{i=1}^{4} f_i = k \sum_{i=1}^{4} \omega_i^2, \quad \boldsymbol{T}^B = \begin{bmatrix} 0 \\ 0 \\ T \end{bmatrix}, \tag{7}$$

$$\boldsymbol{\tau}_B = \begin{bmatrix} \tau_\phi \\ \tau_\theta \\ \tau_\psi \end{bmatrix} = \begin{bmatrix} l\,k\,(-\omega_2^2 + \omega_4^2) \\ l\,k\,(-\omega_1^2 + \omega_3^2) \\ \sum_{i=1}^{4} \tau_{M_i} \end{bmatrix}, \tag{8}$$

in which l is the distance between the rotor and the center of mass of the quadcopter. Thus, the roll movement is acquired by decreasing the 2nd rotor velocity and increasing the 4th rotor velocity. Similarly, the pitch movement is acquired by decreasing the 1st rotor velocity and increasing the 3th rotor velocity. Yaw movement is acquired by increasing the the angular velocities of two opposite rotors and decreasing the velocities of the other two.

2.1 Newton-Euler equations

The quadcopter is assumed to be rigid body and thus Newton-Euler equations can be used to describe its dynamics. In the body frame, the force required for the acceleration of mass $m\dot{\boldsymbol{V}}_B$ and the centrifugal force $\boldsymbol{\nu} \times (m\,\boldsymbol{V}_B)$ are equal to the gravity $\boldsymbol{R}^{\mathrm{T}}\boldsymbol{G}$ and the total thrust of the rotors $\boldsymbol{T}_B$

$$m\dot{\boldsymbol{V}}_B + \boldsymbol{\nu} \times (m\,\boldsymbol{V}_B) = \boldsymbol{R}^{\mathrm{T}}\boldsymbol{G} + \boldsymbol{T}_B. \tag{9}$$

In the inertial frame, the centrifugal force is nullified. Thus, only the gravitational force and the magnitude and direction of the thrust are contributing in the acceleration of the quadcopter

$$m\ddot{\boldsymbol{\xi}} = \boldsymbol{G} + \boldsymbol{R}\,\boldsymbol{T}_B,$$

$$\begin{bmatrix} \ddot{x} \\ \ddot{y} \\ \ddot{z} \end{bmatrix} = -g \begin{bmatrix} 0 \\ 0 \\ 1 \end{bmatrix} + \frac{T}{m} \begin{bmatrix} C_\psi S_\theta C_\phi + S_\psi S_\phi \\ S_\psi S_\theta C_\phi - C_\psi S_\phi \\ C_\theta C_\phi \end{bmatrix}. \tag{10}$$

In the body frame, the angular acceleration of the inertia $\boldsymbol{I}\dot{\boldsymbol{\nu}}$, the centripetal forces $\boldsymbol{\nu} \times (\boldsymbol{I}\boldsymbol{\nu})$ and the gyroscopic forces $\boldsymbol{\Gamma}$ are equal to the external torque $\boldsymbol{\tau}$

$$\boldsymbol{I}\dot{\boldsymbol{\nu}} + \boldsymbol{\nu} \times (\boldsymbol{I}\boldsymbol{\nu}) + \boldsymbol{\Gamma} = \boldsymbol{\tau},$$

$$\dot{\boldsymbol{\nu}} = \boldsymbol{I}^{-1} \left(- \begin{bmatrix} p \\ q \\ r \end{bmatrix} \times \begin{bmatrix} I_{xx}\,p \\ I_{yy}\,q \\ I_{zz}\,r \end{bmatrix} - I_r \begin{bmatrix} p \\ q \\ r \end{bmatrix} \times \begin{bmatrix} 0 \\ 0 \\ 1 \end{bmatrix} \omega_\Gamma + \boldsymbol{\tau} \right), \tag{11}$$

$$\begin{bmatrix} \dot{p} \\ \dot{q} \\ \dot{r} \end{bmatrix} = \begin{bmatrix} (I_{yy} - I_{zz})\,q\,r/I_{xx} \\ (I_{zz} - I_{xx})\,p\,r/I_{yy} \\ (I_{xx} - I_{yy})\,p\,q/I_{zz} \end{bmatrix} - I_r \begin{bmatrix} q/I_{xx} \\ -p/I_{yy} \\ 0 \end{bmatrix} \omega_\Gamma + \begin{bmatrix} \tau_\phi/I_{xx} \\ \tau_\theta/I_{yy} \\ \tau_\psi/I_{zz} \end{bmatrix},$$

in which $\omega_\Gamma = \omega_1 - \omega_2 + \omega_3 - \omega_4$. The angular accelerations in the inertial frame are then attracted from the body frame accelerations with the transformation matrix $\boldsymbol{W}_\eta^{-1}$ and its time derivative

$$\begin{aligned} \ddot{\boldsymbol{\eta}} &= \tfrac{\mathrm{d}}{\mathrm{d}t}\left(\boldsymbol{W}_\eta^{-1}\,\boldsymbol{\nu}\right) = \tfrac{\mathrm{d}}{\mathrm{d}t}\left(\boldsymbol{W}_\eta^{-1}\right)\,\boldsymbol{\nu} + \boldsymbol{W}_\eta^{-1}\,\dot{\boldsymbol{\nu}} \\ &= \begin{bmatrix} 0 & \dot{\phi}C_\phi T_\theta + \dot{\theta}S_\phi/C_\theta^2 & -\dot{\phi}S_\phi C_\theta + \dot{\theta}C_\phi/C_\theta^2 \\ 0 & -\dot{\phi}S_\phi & -\dot{\phi}C_\phi \\ 0 & \dot{\phi}C_\phi/C_\theta + \dot{\phi}S_\phi T_\theta/C_\theta & -\dot{\phi}S_\phi/C_\theta + \dot{\theta}C_\phi T_\theta/C_\theta \end{bmatrix} \boldsymbol{\nu} + \boldsymbol{W}_\eta^{-1}\,\dot{\boldsymbol{\nu}}. \end{aligned} \tag{12}$$

2.2 Euler-Lagrange equations

The Lagrangian $\mathcal{L}$ is the sum of the translational E_{trans} and rotational E_{rot} energies minus potential energy E_{pot}

$$\begin{array}{rcccccc} \mathcal{L}\left(\boldsymbol{q}, \dot{\boldsymbol{q}}\right) & = & E_{trans} & + & E_{rot} & - & E_{pot} \\ & = & (m/2)\, \dot{\boldsymbol{\xi}}^{\mathrm{T}}\, \dot{\boldsymbol{\xi}} & + & (1/2)\, \boldsymbol{\nu}^{\mathrm{T}}\, \boldsymbol{I}\, \boldsymbol{\nu} & - & mgz. \end{array} \tag{13}$$

As shown in [10] the Euler-Lagrange equations with external forces and torques are

$$\left[\begin{array}{c} \boldsymbol{f} \\ \boldsymbol{\tau} \end{array} \right] = \frac{\mathrm{d}}{\mathrm{d}t} \left(\frac{\partial \mathcal{L}}{\partial \dot{\boldsymbol{q}}} \right) - \frac{\partial \mathcal{L}}{\partial \boldsymbol{q}}. \tag{14}$$

The linear and angular components do not depend on each other thus they can be studied separately. The linear external force is the total thrust of the rotors. The linear Euler-Lagrange equations are

$$\boldsymbol{f} = \boldsymbol{R}\boldsymbol{T}_B = m\ddot{\boldsymbol{\xi}} + mg \left[\begin{array}{c} 0 \\ 0 \\ 1 \end{array} \right], \tag{15}$$

which is equivalent with Equation (10).

The Jacobian matrix $\boldsymbol{J}\left(\boldsymbol{\eta}\right)$ from $\boldsymbol{\nu}$ to $\dot{\boldsymbol{\eta}}$ is

$$\begin{array}{c} \boldsymbol{J}\left(\boldsymbol{\eta}\right) = \boldsymbol{J} = \boldsymbol{W}_{\boldsymbol{\eta}}^{\mathrm{T}}\, \boldsymbol{I}\, \boldsymbol{W}_{\boldsymbol{\eta}}, \\ = \left[\begin{array}{ccc} I_{xx} & 0 & -I_{xx} S_\theta \\ 0 & I_{yy} C_\phi^2 + I_{zz} S_\phi^2 & \left(I_{yy} - I_{zz}\right) C_\phi S_\phi C_\theta \\ -I_{xx} S_\theta & \left(I_{yy} - I_{zz}\right) C_\phi S_\phi C_\theta & I_{xx} S_\theta^2 + I_{yy} S_\phi^2 C_\theta^2 + I_{zz} C_\phi^2 C_\theta^2 \end{array} \right]. \end{array} \tag{16}$$

Thus, the rotational energy E_{rot} can be expressed in the inertial frame as

$$E_{rot} = (1/2)\, \boldsymbol{\nu}^{\mathrm{T}}\, \boldsymbol{I}\, \boldsymbol{\nu} = (1/2)\, \ddot{\boldsymbol{\eta}}^{\mathrm{T}}\, \boldsymbol{J}\, \ddot{\boldsymbol{\eta}}. \tag{17}$$

The external angular force is the torques of the rotors. The angular Euler-Lagrange equations are

$$\boldsymbol{\tau} = \boldsymbol{\tau}_B = \boldsymbol{J}\, \ddot{\boldsymbol{\eta}} + \frac{\mathrm{d}}{\mathrm{d}t} \left(\boldsymbol{J} \right)\, \dot{\boldsymbol{\eta}} - \frac{1}{2} \frac{\partial}{\partial \boldsymbol{\eta}} \left(\dot{\boldsymbol{\eta}}^{\mathrm{T}}\, \boldsymbol{J}\, \dot{\boldsymbol{\eta}} \right) = \boldsymbol{J}\, \ddot{\boldsymbol{\eta}} + \boldsymbol{C}\left(\boldsymbol{\eta}, \dot{\boldsymbol{\eta}}\right) \dot{\boldsymbol{\eta}}. \tag{18}$$

,

in which the matrix $\boldsymbol{C}\left(\boldsymbol{\eta}, \dot{\boldsymbol{\eta}}\right)$ is the Coriolis term, containing the gyroscopic and centripetal terms.

The matrix $\boldsymbol{C}\left(\boldsymbol{\eta}, \dot{\boldsymbol{\eta}}\right)$ has the form, as shown in [9],

$$\boldsymbol{C}\left(\boldsymbol{\eta}, \dot{\boldsymbol{\eta}}\right) = \begin{bmatrix} C_{11} & C_{12} & C_{13} \\ C_{21} & C_{22} & C_{23} \\ C_{31} & C_{32} & C_{33} \end{bmatrix},$$

$$\begin{aligned}
C_{11} &= 0 \\
C_{12} &= (I_{yy} - I_{zz})(\dot{\theta}C_\phi S_\phi + \dot{\psi}S_\phi^2 C_\theta) + (I_{zz} - I_{yy})\dot{\psi}C_\phi^2 C_\theta - I_{xx}\dot{\psi}C_\theta \\
C_{13} &= (I_{zz} - I_{yy})\dot{\psi}C_\phi S_\phi C_\theta^2 \\
C_{21} &= (I_{zz} - I_{yy})(\dot{\theta}C_\phi S_\phi + \dot{\psi}S_\phi C_\theta) + (I_{yy} - I_{zz})\dot{\psi}C_\phi^2 C_\theta + I_{xx}\dot{\psi}C_\theta \\
C_{22} &= (I_{zz} - I_{yy})\dot{\phi}C_\phi S_\phi \\
C_{23} &= -I_{xx}\dot{\psi}S_\theta C_\theta + I_{yy}\dot{\psi}S_\phi^2 S_\theta C_\theta + I_{zz}\dot{\psi}C_\phi^2 S_\theta C_\theta \\
C_{31} &= (I_{yy} - I_{zz})\dot{\psi}C_\theta^2 S_\phi C_\phi - I_{xx}\dot{\theta}C_\theta \\
C_{32} &= (I_{zz} - I_{yy})(\dot{\theta}C_\phi S_\phi S_\theta + \dot{\phi}S_\phi^2 C_\theta) + (I_{yy} - I_{zz})\dot{\phi}C_\phi^2 C_\theta \\
&\quad + I_{xx}\dot{\psi}S_\theta C_\theta - I_{yy}\dot{\psi}S_\phi^2 S_\theta C_\theta - I_{zz}\dot{\psi}C_\phi^2 S_\theta C_\theta \\
C_{33} &= (I_{yy} - I_{zz})\dot{\phi}C_\phi S_\phi C_\theta^2 - I_{yy}\dot{\theta}S_\phi^2 C_\theta S_\theta - I_{zz}\dot{\theta}C_\phi^2 C_\theta S_\theta + I_{xx}\dot{\theta}C_\theta S_\theta.
\end{aligned} \tag{19}$$

Equation (18) leads to the differential equations for the angular accelerations which are equivalent with Equations (11) and (12)

$$\ddot{\boldsymbol{\eta}} = \boldsymbol{J}^{-1}\left(\boldsymbol{\tau}_B - \boldsymbol{C}\left(\boldsymbol{\eta}, \dot{\boldsymbol{\eta}}\right)\dot{\boldsymbol{\eta}}\right). \tag{20}$$

2.3 Aerodynamical effects

The preceding model is a simplification of complex dynamic interactions. To enforce more realistical behaviour of the quadcopter, drag force generated by the air resistance is included. This is devised to Equations (10) and (15) with the diagonal coefficient matrix associating the linear velocities to the force slowing the movement, as in [15],

$$\begin{bmatrix} \ddot{x} \\ \ddot{y} \\ \ddot{z} \end{bmatrix} = -g \begin{bmatrix} 0 \\ 0 \\ 1 \end{bmatrix} + \frac{T}{m} \begin{bmatrix} C_\psi S_\theta C_\phi + S_\psi S_\phi \\ S_\psi S_\theta C_\phi - C_\psi S_\phi \\ C_\theta C_\phi \end{bmatrix} - \frac{1}{m} \begin{bmatrix} A_x & 0 & 0 \\ 0 & A_y & 0 \\ 0 & 0 & A_z \end{bmatrix} \begin{bmatrix} \dot{x} \\ \dot{y} \\ \dot{z} \end{bmatrix}, \tag{21}$$

in which A_x, A_y and A_z are the drag force coefficients for velocities in the corresponding directions of the inertial frame.

Several other aerodynamical effects could be included in the model. For example, dependence of thrust on angle of attack, blade flapping and airflow distruptions have been studied in [1] and [2]. The influence of aerodynamical effects are complicated and the effects are difficult to model. Also some of the effects have significant effect only in high velocities. Thus, these effects are excluded from the model and the presented simple model is used.

3 Simulation

The mathematical model of the quadcopter is implemented for simulation in Matlab 2010 with Matlab programming language. Parameter values from [3] are used in the simulations and are presented in Table 1. The values of the drag force coefficients A_x, A_y and A_z are selected such as the quadcopter will slow down and stop when angles ϕ and θ are stabilised to zero values.

Table 1: Parameter values for simulation

Parameter	Value	Unit
g	9.81	$\mathrm{m/s^2}$
m	0.468	kg
l	0.225	m
k	$2.980 \cdot 10^{-6}$	
b	$1.140 \cdot 10^{-7}$	
I_M	$3.357 \cdot 10^{-5}$	$\mathrm{kg\ m^2}$

Parameter	Value	Unit
I_{xx}	$4.856 \cdot 10^{-3}$	$\mathrm{kg\ m^2}$
I_{yy}	$4.856 \cdot 10^{-3}$	$\mathrm{kg\ m^2}$
I_{zz}	$8.801 \cdot 10^{-3}$	$\mathrm{kg\ m^2}$
A_x	0.25	kg/s
A_y	0.25	kg/s
A_z	0.25	kg/s

The mathematical model is tested by simulating a quadcopter with an example case as following. The quadcopter is initially in a stable state in which the values of all positions and angles are zero, the body frame of the quadcopter is congruent with the inertial frame. The total thrust is equal to the hover thrust, the thrust equal to gravity. The simulation progresses at 0.0001 second intervals to total elapsed time of two seconds. The control inputs, the angular velocities of the four rotors, are shown in Figure 2, the inertial positions x, y and z in Figure 3, and the angles ϕ, θ and ψ in Figure 4.

For the first 0.25 seconds the quadcopter ascended by increasing all of the rotor velocities from the hover thrust. Then, the ascend is stopped by decreasing the rotor velocities significantly for the following 0.25 seconds. Consequently the quadcopter ascended 0.1 meters in the first 0.5 seconds. After the ascend the quadcopter is stable again.

Next the quadcopter is put into a roll motion by increasing the velocity of the fourth rotor and decreasing the velocity of the second rotor for 0.25 seconds. The acceleration of the roll motion is stopped by decreasing the velocity of the fourth and increasing the velocity of the second rotor for 0.25 seconds. Thus, after 0.5 seconds in roll motion the roll angle ϕ had increased approx. 25 degrees. Because of the roll angle the quadcopter accelerated in the direction of the negative y-axis.

Then, similar to the roll motion, a pitch motion is created by increasing the velocity of the third rotor and decreasing the velocity of the first. The motion is stopped by decreasing the velocity of the third rotor and increasing the velocity of the first rotor. Due to the pitch movement, the pitch angle θ had increased approximately

22 degrees. The acceleration of the quadcopter in the direction of the positive x-axis is caused by the pitch angle.

Finally, the quadcopter is turned in the direction of the yaw angle ψ by increasing the velocities of the first and the third rotors and decreasing the velocities of the second and the fourth rotors. The yaw motion is stopped by decreasing the velocities of the first and the third rotors and increasing the velocities of the second and the fourth rotors. Consequently the yaw angle ψ increases approximately 10 degrees.

During the whole simulation the total thrust of the rotors had remained close to the initial total thrust. Thus, the deviations of the roll and pitch angles from the zero values decrease the value of the thrust in the direction of the z-axis. Consequently the quadcopter accelerates in the direction of the negative z-axis and is descending.

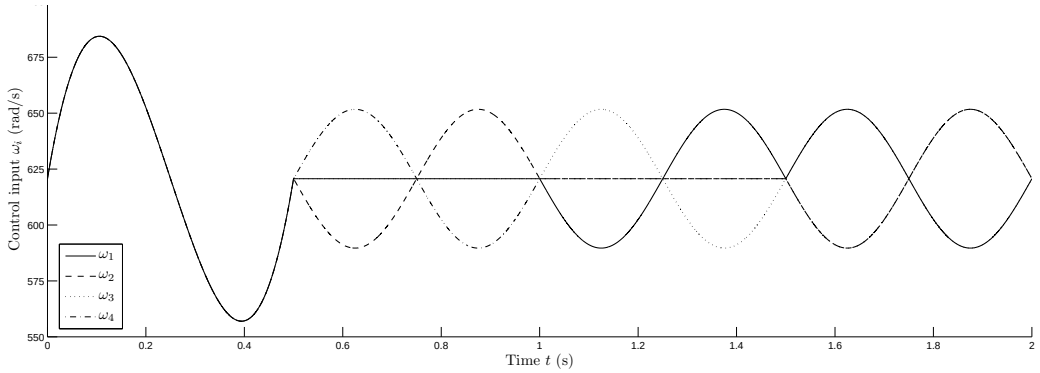

Figure 2: Control inputs ω_i

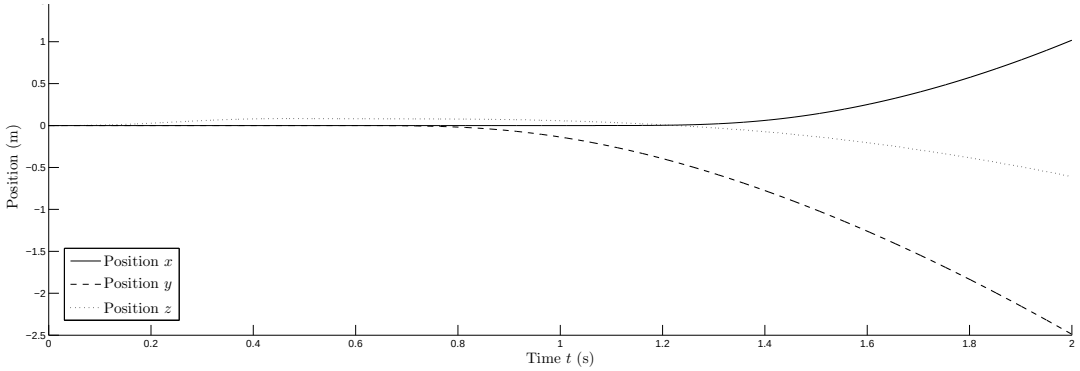

Figure 3: Positions x, y, and z

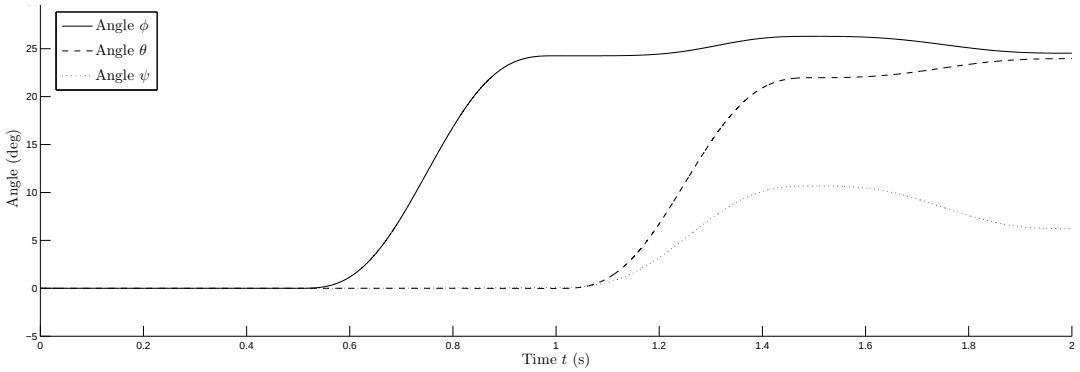

Figure 4: Angles ϕ, θ, and ψ

4 Stabilisation of quadcopter

To stabilise the quadcopter, a PID controller is utilised. Advantages of the PID controller are the simple structure and easy implementation of the controller. The general form of the PID controller is

$$\begin{aligned} e(t) &= x_d(t) - x(t), \\ u(t) &= K_P\, e(t) + K_I \int_0^t e(\tau)\; d\,\tau + K_D \frac{\mathrm{d}\, e(t)}{\mathrm{d}\, t}, \text{ [16]} \end{aligned} \tag{22}$$

in which $u(t)$ is the control input, $e(t)$ is the difference between the desired state $x_d(t)$ and the present state $x(t)$, and K_P, K_I and K_D are the parameters for the proportional, integral and derivative elements of the PID controller.

In a quadcopter, there are six states, positions $\boldsymbol{\xi}$ and angles $\boldsymbol{\eta}$, but only four control inputs, the angular velocities of the four rotors ω_i. The interactions between the states and the total thrust T and the torques $\boldsymbol{\tau}$ created by the rotors are visible from the quadcopter dynamics defined by Equations (10), (11), and (12). The total thrust T affects the acceleration in the direction of the z-axis and holds the quadcopter in the air. Torque τ_ϕ has an affect on the acceleration of angle ϕ, torque τ_θ affects the acceleration of angle θ, and torque τ_ψ contributes in the acceleration of angle ψ.

Hence, the PD controller for the quadcopter is chosen as, similarly as in [4],

$$\begin{aligned} T &= \left(g + K_{z,D}\left(\dot{z_d} - \dot{z}\right) + K_{z,P}\left(z_d - z\right)\right) \frac{m}{C_\phi C_\theta}, \\ \tau_\phi &= \left(K_{\phi,D}\left(\dot{\phi_d} - \dot{\phi}\right) + K_{\phi,P}\left(\phi_d - \phi\right)\right) I_{xx}, \\ \tau_\theta &= \left(K_{\theta,D}\left(\dot{\theta_d} - \dot{\theta}\right) + K_{\theta,P}\left(\theta_d - \theta\right)\right) I_{yy}, \\ \tau_\psi &= \left(K_{\psi,D}\left(\dot{\psi_d} - \dot{\psi}\right) + K_{\psi,P}\left(\psi_d - \psi\right)\right) I_{zz}, \end{aligned} \tag{23}$$

in which also the gravity g, and mass m and moments of inertia $\boldsymbol{I}$ of the quadcopter are considered.

The correct angular velocities of rotors ω_i can be calculated from Equations (7) and (8) with values from Equation (23)

$$\begin{aligned} \omega_1^2 &= \frac{T}{4k} - \frac{\tau_\theta}{2kl} - \frac{\tau_\psi}{4b} \\ \omega_2^2 &= \frac{T}{4k} - \frac{\tau_\phi}{2kl} + \frac{\tau_\psi}{4b} \\ \omega_3^2 &= \frac{T}{4k} + \frac{\tau_\theta}{2kl} - \frac{\tau_\psi}{4b} \\ \omega_4^2 &= \frac{T}{4k} + \frac{\tau_\phi}{2kl} + \frac{\tau_\psi}{4b} \end{aligned} \tag{24}$$

The performance of the PD controller is tested by simulating the stabilisation of a quadcopter. The PD controller parameters are presented in Table 2. The initial condition of the quadcopter is for position $\boldsymbol{\xi} = [0\ 0\ 1]^{\mathrm{T}}$ in meters and for angles

$\boldsymbol{\eta} = [10\ 10\ 10]^{\mathrm{T}}$ in degrees. The desired position for altitude is $z_d = 0$. The purpose of the stabilisation is stable hovering, thus $\boldsymbol{\eta}_d = [0\ 0\ 0]^{\mathrm{T}}$.

Table 2: Parameters of the PD controller

Parameter	Value	Parameter	Value
$K_{z,D}$	2.5	$K_{z,P}$	1.5
$K_{\phi,D}$	1.75	$K_{\phi,P}$	6
$K_{\theta,D}$	1.75	$K_{\theta,P}$	6
$K_{\psi,D}$	1.75	$K_{\psi,P}$	6

The control inputs ω_i, the positions $\boldsymbol{\xi}$ and the angles $\boldsymbol{\eta}$ during the simulation are presented in Figures 5, 6, and 7. The altitude and the angles are stabilised to zero value after 5 seconds. However, the positions x and y deviated from the zero values because of the non-zero values of the angles. Before the quadcopter is stabilised to hover, it has already moved over 1 meters in the direction of the positive x axis and 0,5 meters in the direction of the negative y axis. This is because the control method of the PD contoller does not consider the accelerations in the directions of x and y. Thus, another control method should be constructed to give a control on all of positions and angles of the quadcopter.

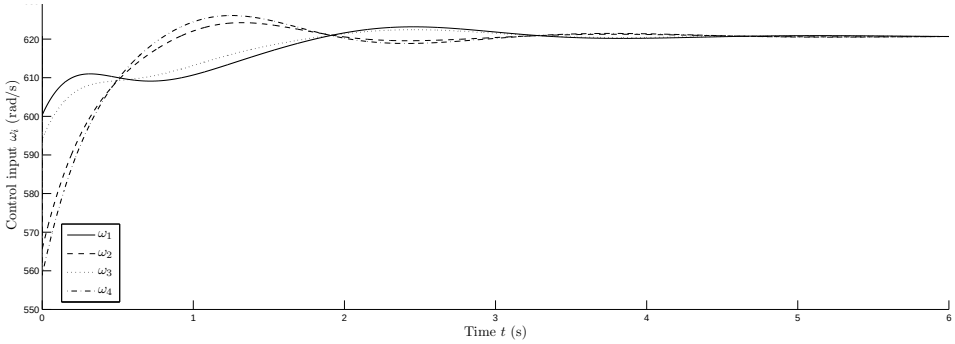

Figure 5: Control inputs ω_i

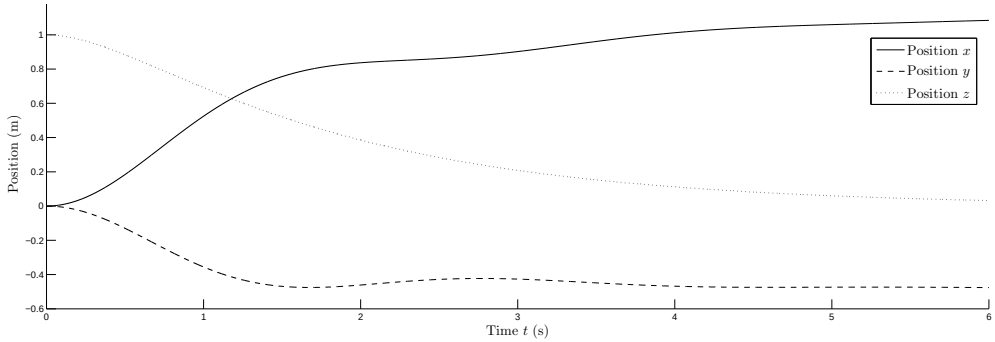

Figure 6: Positions x, y, and z

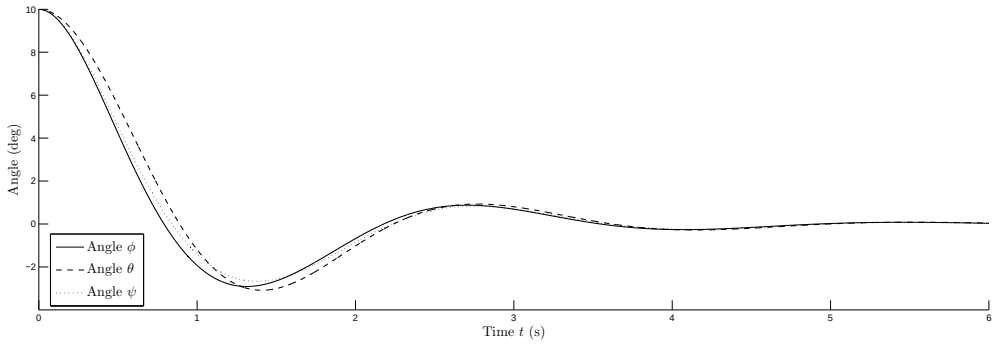

Figure 7: Angles ϕ, θ, and ψ

5 Trajectory control

The purpose of trajectory control is to move the quadcopter from the original location to the desired location by controlling the rotor velocities of the quadcopter. Finding optimal trajectory for a quadcopter is a difficult task because of complex dynamics. However, a simple control method is able to control the quadcopter adequately. Thus, a heuristic approach is studied and developed here.

The basis of the development of a control method is the study of the interactions and dependances between states, state derivatives and control inputs. These interactions and dependances are defined by Equations (7), (8), (20) and (21) and presented in Figure 8.

The given control inputs ω_i define the total thrust T and the torques τ_ϕ, τ_θ and τ_ψ. The torques affect the angular accelerations depending on the current angles and angular velocities. The angles $\boldsymbol{\eta}$ can be integrated from the angular velocities $\dot{\boldsymbol{\eta}}$, which are integrated from the angular accelerations $\ddot{\boldsymbol{\eta}}$. The linear accelerations $\ddot{\boldsymbol{\xi}}$ depend on the total thrust T, the angles $\boldsymbol{\eta}$ and the linear velocities $\dot{\boldsymbol{\xi}}$. The linear position $\boldsymbol{\xi}$ is integrated from the linear accelerations $\ddot{\boldsymbol{\xi}}$ through the linear velocities $\dot{\boldsymbol{\xi}}$.

Hence, to find proper control inputs ω_i for given states $\boldsymbol{\xi}$ this line of thought has to be done in reverse.

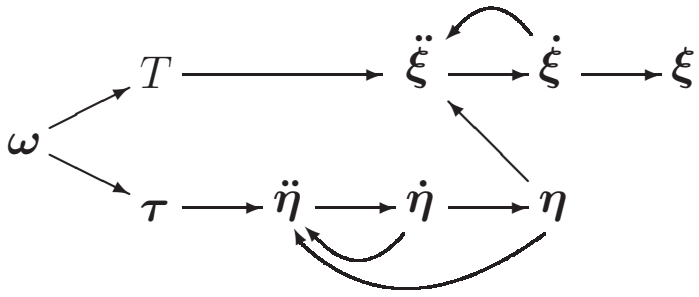

Figure 8: Interactions between states, state derivatives, and control inputs

One method is to generate linear accelerations which accomplish the wanted trajectory according to positions x, y and z for each time t. From Equation (21), three equations are received

$$\boldsymbol{T}_B = \begin{bmatrix} 0 \\ 0 \\ T \end{bmatrix} = \boldsymbol{R}^{\mathrm{T}} \left(m \left(\ddot{\boldsymbol{\xi}} + \begin{bmatrix} 0 \\ 0 \\ g \end{bmatrix} \right) + \begin{bmatrix} A_x & 0 & 0 \\ 0 & A_y & 0 \\ 0 & 0 & A_z \end{bmatrix} \dot{\boldsymbol{\xi}} \right). \tag{25}$$

in which $\ddot{\boldsymbol{\xi}}$, $\dot{\boldsymbol{\xi}}$, and ψ are desired trajectory values as well as angles ϕ and θ and total thrust T are unknown values to be solved.

From this equation, the required angles ϕ and θ and the total thrust T for each time t can be calculated, as shown in [5],

$$\phi = \arcsin\left(\frac{d_x\, S_\psi - d_y\, C_\psi}{d_x^2 + d_y^2 + (d_z + g)^2}\right),$$
$$\theta = \arctan\left(\frac{d_x\, C_\psi + d_y\, S_\psi}{d_z + g}\right), \tag{26}$$
$$T = m\,(d_x\ (S_\theta C_\psi C_\phi + S_\psi S_\phi) + d_y\ (S_\theta S_\psi C_\phi - C_\psi S_\phi) + (\,d_z + g\,)\, C_\theta C_\phi)\,,$$

in which

$$\begin{aligned} d_x &= \ddot{x} + A_x\dot{x}/m, \\ d_y &= \ddot{y} + A_y\dot{y}/m, \\ d_z &= \ddot{z} + A_z\dot{z}/m. \end{aligned} \tag{27}$$

When the values of the angles ϕ and θ are known, the angular velocities and accelerations can be calculated from them with simple derivation. With the angular velocities and accelerations, the torques $\boldsymbol{\tau}$ can be solved from Equation (20). When the torques and thrust are known, the control inputs ω_i can be calculated from Equation (24).

5.1 Heuristic method for trajectory generation

The generation of proper accelerations $\ddot{\boldsymbol{\xi}}$ is difficult because the composition of the third and fourth derivatives of the position, jerk and jounce, has to be reasonable. The influence of the jounce values is visible in the composition of the control inputs ω_i. High jounce values will mean high control input values and thus the jounces have to be considered closely when generating the accelerations.

A heuristic method can be used to generate jounce values. The method utilises a symmetric structure in jouce function $f(t)$ to control the derivatives. One influencial part of the function is defined by three sine functions as following

$$f(t) = \begin{cases} a\sin\left(\frac{1}{b}\,\pi\,t\right), & 0 \le t \le b, \\ -a\sin\left(\frac{1}{b}\,\pi\,t - \pi\right), & b \le t \le 3b, \\ a\sin\left(\frac{1}{b}\,\pi\,t - 3\pi\right), & 3b \le t \le 4b. \end{cases} \tag{28}$$

The structure of the function is visualised in Figure 9. The sine functions are used to give a smooth function. These three sine functions form a function in which the first half increases acceleration to certain value and then the second half of the function decreases it back to zero. This acceleration generates constant velocity. Mirror image of the function can be used to decelerate the velocity back to zero. The final position depends on the parameters a and b of the sine functions, presented

in Equation (28), and the time c between the accelerating part and the decelerating part, the mirror image, of the jounce.

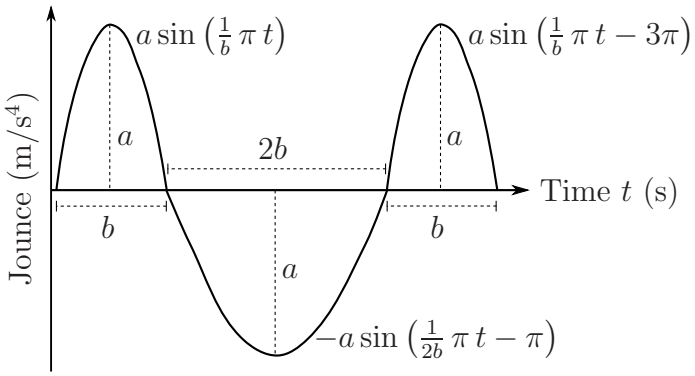

Figure 9: Heuristic method for the generation of jounce functions

Unfortunately, the method does not give optimal trajectories. Thus, a dynamic optimisation model and a suitable algorithm would be needed to calculate optimally the trajectory of the quadcopter. However, the method presented is easy to use to generate proper values of jounce which will achieve the wanted trajectory.

The functionality of the method is studied with an example simulation. Jounce of position x is created according to Equation (28) with parameters $a = 1$, $b = 0.5$ and $c = 2$. The position x and its derivatives derived from the planned jounce are presented in Figure 10. The jounce could also be generated simultaneously for y and z. However, in this example, only position x is considered because the relationship between the jounce of position x and the control inputs ω_1 and ω_3, controlling the angle θ, is more visible.

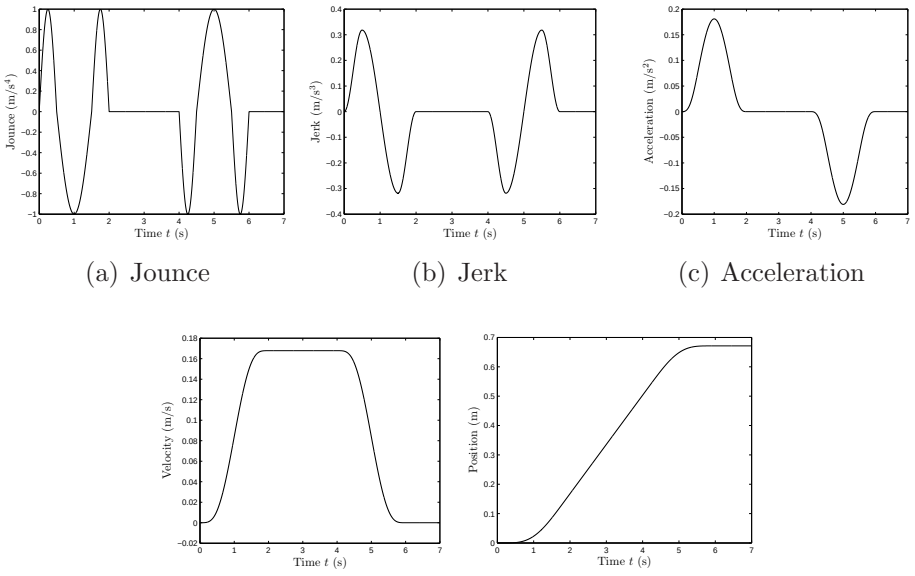

(a) Jounce (b) Jerk (c) Acceleration

(d) Velocity (e) Position

Figure 10: Planned position x and its derivatives with given jounce

The simulation of the example case is performed with previously given accelerations and velocities of position x. The planned value of angle ψ is zero for each time t. First, the required angles ϕ and θ and thrust T are solved from Equation (26) for each time t. The angular velocities and accelerations are calculated from the solved angles with derivation. Then, the torques are solved using the angular velocities and accelerations. Finally, the control inputs are solved. Then, the simulation is performed with given control inputs.

The calculated control inputs are presented in Figure 11. The simulated positions $\boldsymbol{\xi}$ are presented in Figure 12 and the simulated angles $\boldsymbol{\eta}$ in Figure 13. According to Figure 12, the simulated position x is the same as the planned position x in Figure 10(e) and the values of the positions y and z stay as zeroes. The angle θ increases during the acceleration and then stabilises to a constant value to generate the constant acceleration required to compensate the drag force caused by the planned constant velocity. Finally, the angle is changed to the opposite direction to decelerate the quadcopter to a halt.

The shape of the calculated control inputs ω_1 and ω_3 in Figure 11 are similar to planned jounce in Figure 10(a). The shape of the simulated angle θ follows the shape of the planned acceleration $\ddot{x}$. The shapes of the control inputs and the angles differ from the planned values of the jounce and the acceleration because the drag force, caused by the velocity, has to be compensated.

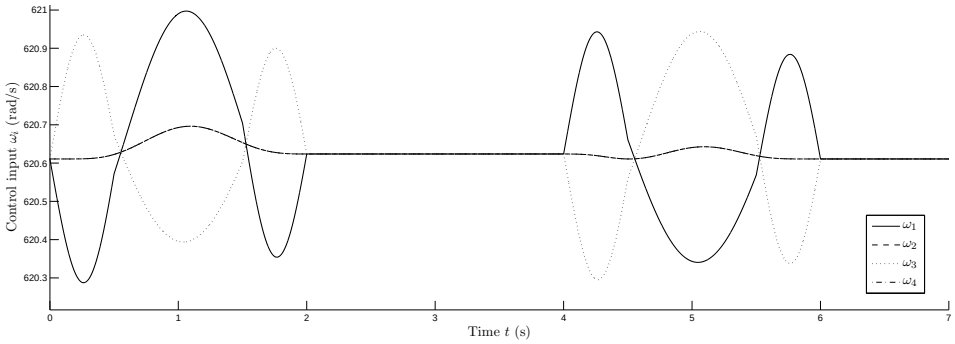

Figure 11: Control inputs ω_i

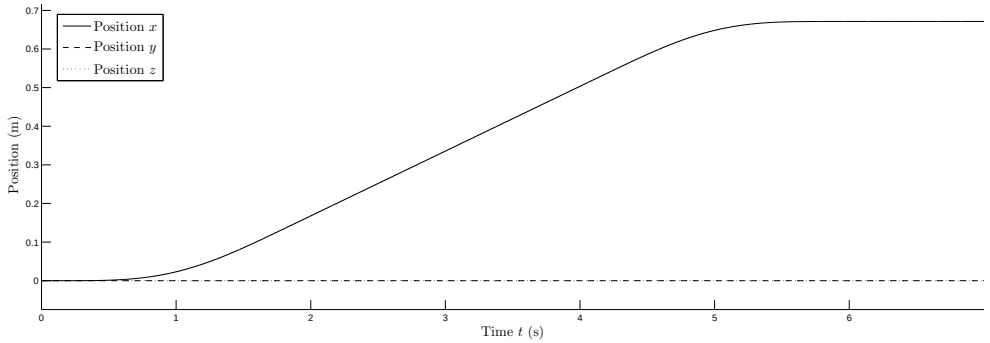

Figure 12: Positions x, y, and z

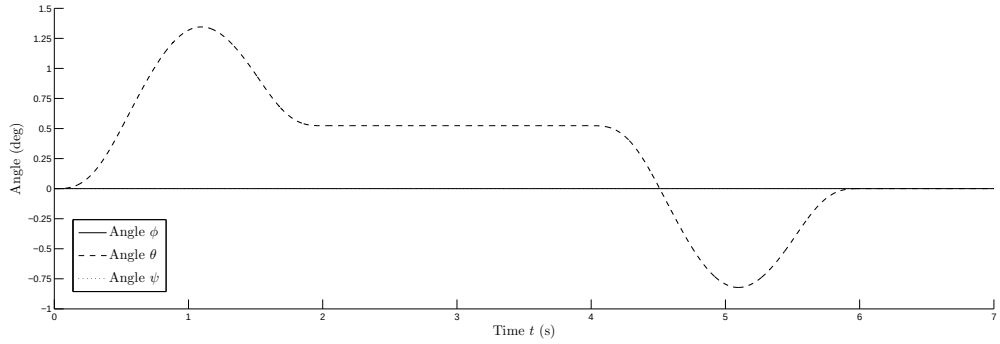

Figure 13: Angles ϕ, θ, and ψ

The method can also be used even if there are unmodeled linear forces, wind for example, which affect the linear accelerations and consequently the position of the quadcopter. If the trajectory is calculated in shorter distances, it is possible to correct the trajectory with new calculation from the current, but inaccurate, location to the next checkpoint. Example of this method is presented in Figure 14. The arrows with dash lines indicate the planned trajectory in the x, y-plane and the solid arrows indicate the realised trajectory. The black squares mark the start and the finish positions and the white squares mark the checkpoints for the trajectory.

The control inputs are calculated from the current location of the quadcopter to the next checkpoint but because of random and unmodelled forces the realised position, marked with X, differs from the planned. If the quadcopter is close enough to the target checkpoint, the target checkpoint is changed to the next one and new control inputs are calculated. After repeating this and going through all of the checkpoints, the quadcopter reaches the final destination.

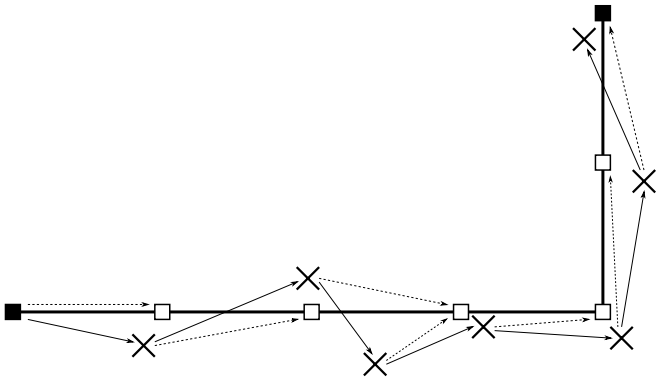

Figure 14: Example of checkpoint flight pattern with external disturbances

The biggest weakness in the proposed method is that it works as shown only if the quadcopter starts from a stable attitude, the angles ϕ and θ and their derivatives are zeros, and there are no external forces influencing the attitude during the flight. Small deviations in the angles can result into a huge deviation in the trajectory. One way to solve this problem is to stabilise the quadcopter at each checkpoint with a PD controller proposed earlier or by using the heuristic method to angles. However, if the angular disturbances are continuous, the benefit from temporary stabilisation is only momentary.

5.2 Integrated PD controller

Another method to take into account the possible deviations in the angles, is to integrate a PD controller into the heuristic method. This is a simplified version of the proposed control method in [5]. The required values d_x, d_y, and d_z in Equation (26) are given by the PD controller considering the deviations between the current and desired values (subscript d) of the positions $\boldsymbol{\xi}$, velocities $\dot{\boldsymbol{\xi}}$, and accelerations $\ddot{\boldsymbol{\xi}}$.

$$\begin{aligned} d_x &= K_{x,P}\,(x_d - x) + K_{x,D}\,(\dot{x}_d - \dot{x}) + K_{x,DD}\,(\ddot{x}_d - \ddot{x})\,, \\ d_y &= K_{y,P}\,(y_d - y) + K_{y,D}\,(\dot{y}_d - \dot{y}) + K_{y,DD}\,(\ddot{y}_d - \ddot{y})\,, \\ d_z &= K_{z,P}\,(z_d - z) + K_{z,D}\,(\dot{z}_d - \dot{z}) + K_{z,DD}\,(\ddot{z}_d - \ddot{z})\,. \end{aligned} \tag{29}$$

Then, the commanded angles ϕ_c and θ_c and thrust T are given by Equation (26). The torques $\boldsymbol{\tau}$ are controlled by the PD controller in Equation (30), same as in

Equation (23). The control inputs can be solved with the calculated thrust and torques by using Equation (24)

$$\begin{aligned} \tau_\phi &= \left(K_{\phi,P}\left(\phi_c - \phi\right) + K_{\phi,D}\left(\dot{\phi}_c - \dot{\phi}\right)\right) I_{xx}, \\ \tau_\theta &= \left(K_{\theta,P}\left(\theta_c - \theta\right) + K_{\theta,D}\left(\dot{\theta}_c - \dot{\theta}\right)\right) I_{yy}, \\ \tau_\psi &= \left(K_{\psi,P}\left(\psi_d - \psi\right) + K_{\psi,D}\left(\dot{\psi}_d - \dot{\psi}\right)\right) I_{zz}. \end{aligned} \tag{30}$$

The performance of the PD controller is demonstrated with an example case in which for all positions x, y and z and their derivatives the values are same as in Figure 10. The simulation is performed with the PD parameters presented in Table 3.

Table 3: Parameters of the PD controller

Variable	Parameter value		
i	$K_{i,P}$	$K_{i,D}$	$K_{i,DD}$
x	1.85	0.75	1.00
y	8.55	0.75	1.00
z	1.85	0.75	1.00
ϕ	3.00	0.75	-
θ	3.00	0.75	-
ψ	3.00	0.75	-

The results of the simulation are presented Figures 15 - 17. The simulated control inputs are presented in Figure 15, the simulated positions in Figure 16 and the simulated angles in Figure 17. The position of the quadcopter is close to the planned position after 6 seconds but the position keeps fluctuating close to the planned values for several seconds. The angles variate greatly during the simulation to achieve the wanted positions, velocities, and accelerations. The values of the control inputs oscillated during the acceleration but then their behaviour became more stable.

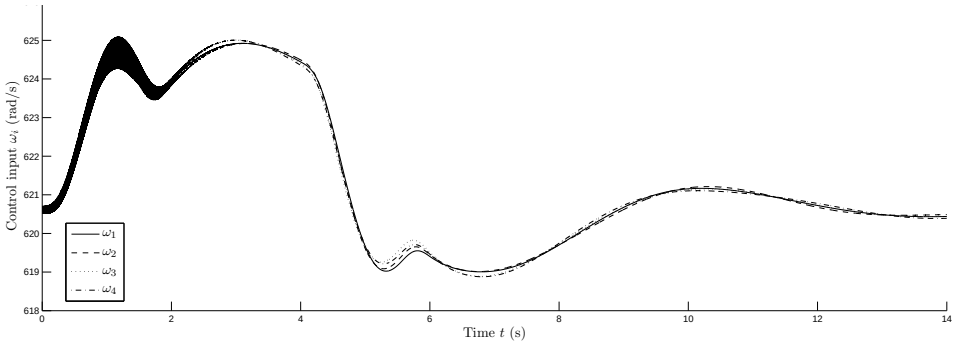

Figure 15: Control inputs ω_i

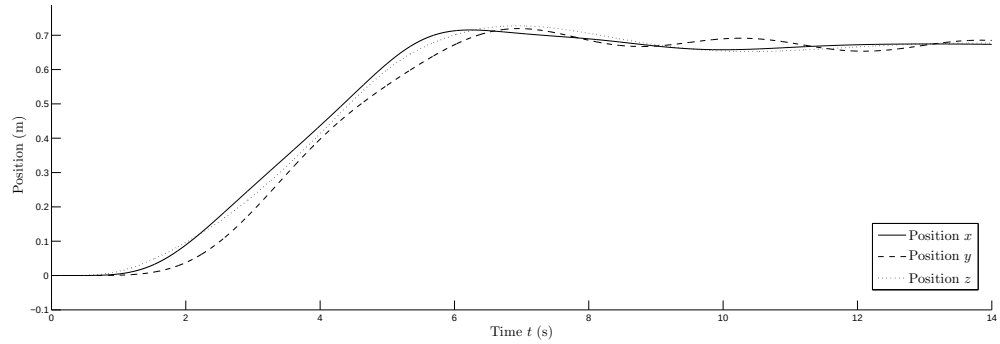

Figure 16: Positions x, y, and z

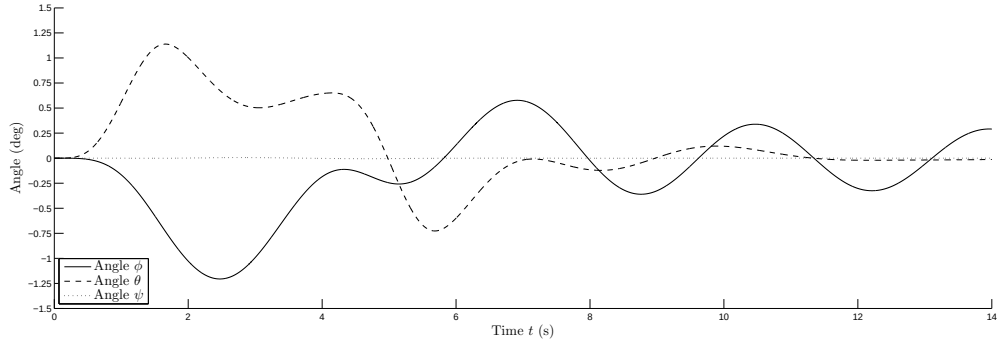

Figure 17: Angles ϕ, θ, and ψ

The proposed integrated PD controller performed well in the example case. However, the performance of the controller is highly depended on the parameter values. If the parameter values are small, the controller will not respond quickly enough to follow the planned trajectory. If the parameter values are substantial, the quadcopter can not perform the required drastic changes in the angular velocities of the rotor and the control inputs, calculated from Equation (24), can be infeasible with certain torques. Thus, the use of equations considering the torques and the control inputs requires a method to calculate the best feasible torques, and from them the best control inputs. Another possible method would be to variate the PD parameters according to the current positions and angles and their derivatives but it is extremely difficult.

6 Conclusion

This paper studied mathematical modelling and control of a quadcopter. The mathematical model of quadcopter dynamics was presented and the differential equations were derived from the Newton-Euler and the Euler-Lagrange equations. The model was verified by simulating the flight of a quadcopter with Matlab. Stabilisation of attitude of the quadcopter was done by utilising a PD controller. A heuristic method was developed to control the trajectory of the quadcopter. The PD contoller was integrated into the heuristic method for better response to disturbances in the flight conditions of the quadcopter.

The simulation proved the presented mathematical model to be realistic in modelling the position and attitude of the quadcopter. The simulation results also showed that the PD controller was efficient in stabilising the quadcopter to the desired altitude and attitude. However, the PD controller did not considered positions x and y. Thus, the values of x and y variated from their original values during the stabilisation process. This was a result of the deviation of the roll and pitch angles from zero values.

According to the simulation results, the proposed heuristic method produced good flight trajectories. The heuristic method required only three parameters to generate the values for the jounce of the position. The position and its other derivatives were calculated from the jounce values. The total thrust and the pitch and roll angles to achieve given accelerations were solved from the linear differential equations. Then, the torques were determined by the angular accelerations and angular velocities calculated from the angles. Finally, the required control inputs were solved from the total thrust and the torques. The simulation results indicated that the quadcopter could be controlled accurately with the control inputs given by the method.

The proposed heuristic method does not consider unmodelled disturbances, such as wind, and thus the PD controller was integrated into the control method. The integrated PD controller operated well in the example simulation. The quadcopter followed the given trajectory and began to stabilise after reaching the final destination. However, the PD controller can perform poorly if the parameter values are not properly selected and are too small or high.

The presented mathematical model only consists of the basic structures of the quadcopter dynamics. Several aerodynamical effects were excluded which can lead to unrealiable behaviour. Also the electric motors spinning the fours rotors were not modelled. The behaviour of a motor is easily included in the model but would require estimation of the parameter values of the motor. The position and attitude information was assumed to be accurate in the model and the simulations. However, the measuring devices in real life are not perfectly accurate as random variations and errors occur. Hence, the effects of imprecise information to the flight of the quadcopter should be studied as well. Also methods to enhance the accuracy of the measurements should be researched and implemented to improve all aspects required

for robust quadcopter manoeuvres.

The presented model and control methods were tested only with simulations. Real experimental prototype of a quadcopter should be constructed to achieve more realistic and reliable results. Even though the construction of a real quadcopter and the estimation of all the model parameters are laborious tasks, a real quadcopter would bring significant benefits to the research. With a real propotype, the theoretical framework and the simulation results could be compared to real-life measurements. This paper did not include these higlighted matters in the study but presented the basics of quadcopter modelling and control. This paper can thus be used as a stepping-stone for future research in more complex modelling of the quadcopter.

References

[1] G. M. Hoffmann, H. Huang, S. L. Waslander, and C. J. Tomlin, "Quadrotor helicopter flight dynamics and control: Theory and experiment," *Proceedings of the AIAA Guidance, Navigation and Control Conference and Exhibit*, Aug. 2007.

[2] H. Huang, G. M. Hoffmann, S. L. Waslander, and C. J. Tomlin, "Aerodynamics and control of autonomous quadrotor helicopters in aggressive maneuvering," *IEEE International Conference on Robotics and Automation*, pp. 3277–3282, May 2009.

[3] A. Tayebi and S. McGilvray, "Attitude stabilization of a four-rotor aerial robot," *43rd IEEE Conference on Decision and Control*, vol. 2, pp. 1216–1221, 2004.

[4] İ. C. Dikmen, A. Arısoy, and H. Temeltaş, "Attitude control of a quadrotor," *4th International Conference on Recent Advances in Space Technologies*, pp. 722–727, 2009.

[5] Z. Zuo, "Trajectory tracking control design with command-filtered compensation for a quadrotor," *IET Control Theory Appl.*, vol. 4, no. 11, pp. 2343–2355, 2010.

[6] S. Bouabdallah, A. Noth, and R. Siegwart, "PID vs LQ control techniques applied to an indoor micro quadrotor," *IEEE/RSJ International Conference on Intelligent Robots and Systems*, vol. 3, pp. 2451–2456, 2004.

[7] T. Madani and A. Benallegue, "Backstepping control for a quadrotor helicopter," *IEEE/RSJ International Conference on Intelligent Robots and Systems*, pp. 3255–3260, 2006.

[8] K. M. Zemalache, L. Beji, and H. Marref, "Control of an under-actuated system: Application to a four rotors rotorcraft," *IEEE International Conference on Robotic and Biomimetics*, pp. 404–409, 2005.

[9] G. V. Raffo, M. G. Ortega, and F. R. Rubio, "An integral predictive/nonlinear $\mathcal{H}_\infty$ control structure for a quadrotor helicopter," *Automatica*, vol. 46, no. 1, pp. 29–39, 2010.

[10] P. Castillo, R. Lozano, and A. Dzul, "Stabilisation of a mini rotorcraft with four rotors," *IEEE Control Systems Magazine*, pp. 45–55, Dec. 2005.

[11] J. Escareño, C. Salazar-Cruz, and R. Lozano, "Embedded control of a four-rotor UAV," *American Control Conference*, vol. 4, no. 11, pp. 3936–3941, 2006.

[12] P. Martin and E. Salaün, "The true role of acceleromter feedback in quadrotor control," *IEEE International Conference on Robotics and Automation*, pp. 1623–1629, May 2010.

[13] R. He, S. Prentice, and N. Roy, "Planning in information space for a quadrotor helicopter in a GPS-denied environment," *IEEE International Conference on Robotics and Automation*, pp. 1814–1820, 2008.

[14] T. S. Alderete, "Simulator aero model implementation." NASA Ames Research Center, Moffett Field, California, `http://www.aviationsystemsdivision.arc.nasa.gov/publications/hitl/rtsim/Toms.pdf`.

[15] H. Bouadi and M. Tadjine, "Nonlinear observer design and sliding mode control of four rotors helicopter," *Proceedings of World Academy of Science, Engineering and Technology*, vol. 25, pp. 225–230, 2007.

[16] K. J. Åström and T. Hägglund, *Advanced PID Control*. ISA - Instrumentation, Systems and Automation Society, 2006.